Surface segregation effect for transition-metal alloys in the coherent-potential approximation: general considerations and calculations for Cu-Ni alloys

1990 J. Phys.: Condens. Matter 2 869

(http://iopscience.iop.org/0953-8984/2/4/008)

J. Phys.: Condens. Matter 2 (1990) 869–885. Printed in the UK

Surface segregation effect for transition-metal alloys in the coherent-potential approximation: general considerations and calculations for Cu–Ni alloys

M Brejnak and P Modrak
Institute of Physical Chemistry of the Polish Academy of Sciences, Kasprzaka 44/52, 01-224 Warsaw, Poland

Received 26 May 1989, in final form 21 August 1989

Abstract. The surface segregation is calculated in the coherent-potential approximation. The influence of the surface potential, d-band fillings and d-level splitting of alloy components on the segregation is examined for a model density of states. The realistic tight-binding Hamiltonian is used to calculate the segregation for Cu–Ni alloys. The model for all reasonable values of parameters predicts the segregation of copper for all alloy compositions.

1. Introduction

The surface segregation effect, i.e. an enrichment of the surface layer with one of the components of the alloy, is reported or predicted for most binary transition-metal alloys [1, 2]. The correlation of the phenomenological properties of the alloy, such as the heat of solution, the difference in the pure metal surface energies and the elastic size mismatch, with the surface segregation and its calculations based on pairwise atomic interactions have been the subject of many papers (cf [1, 3–17] and references therein). On the other hand, fewer attempts to correlate the surface segregation with electronic properties of alloys are reported in the literature [18–30]. The main purpose of the present paper is to improve the calculation of the electronic contribution to the free energy of the system. The model assumed is based on the coherent-potential approximation (CPA) in its classical form [31, 32]. The improved version of CPA used in [18] has required subsequent approximations in the calculation of the segregation. Because of that, the method has led for the bulk crystal to a CPA equation identical with that obtained in [32] for a semi-circle model density of states and has introduced uncontrolled approximations for the surface density of states of the alloy.

On the assumption that the surface affects the s bands of both constituents of the alloy in similar way, the driving force for the segregation of one component of the transition-metal alloy can be ascribed to changes in the d-electron band due to the presence of the surface [19]. At the present stage of calculations the s-band contribution is completely neglected.

The paper is arranged in the following way. In § 2 the method of calculation is presented, a simple Hamiltonian is introduced and approximations going beyond the CPA are discussed. It is shown that calculations of the surface segregation can be performed at

0953-8984/90/040869 + 17 $03.50

various levels of accuracy both in the case of the simple Hamiltonian considered in this section and in the case of realistic densities of states of alloy components considered in § 4. Section 3 contains the results of simple model calculations. The aim of these calculations is to illustrate the influence of the surface potential on the segregation and to show that the model based on d-band contributions of alloy components can lead to different behaviours of the surface segregation as a function of bulk composition depending on the parameters of the model.

In § 4 the calculation for the realistic density of states of Cu–Ni alloys is reported. Because of its importance as a catalyst, many experimental [33–46] and theoretical [1, 4–19, 21–30] studies have been devoted to determining the surface composition of the alloy. The present work in comparison with the previous similar approaches [18, 23, 28, 30] makes progress in two respects.

(i) The surface potential is incorporated into the theory of the surface segregation.
(ii) Realistic densities of states of the alloy components are used in the calculation.

The surface segregation in Cu–Ni alloys particularly for large Cu concentrations has recently become a subject of great interest because of the crossover phenomenon which is reported in both experimental [44] and theoretical [28] papers and is questioned by others [29, 30, 45]. The present paper seems to throw some light on the problem from the point of view of the microscopic electronic theory of the surface segregation.

Section 5 contains the summary and the conclusions.

2. Method of calculation

The calculations of the surface segregation are based on the following assumptions.

(i) The transition metals considered form a disordered binary substitutional alloy.
(ii) The segregation depends mainly on the d-band properties of the components A and B of the alloy.

The free energy per atom for the random alloy can be approximately written in the form [18]

$$F = \frac{1}{N}\sum_{i=1}^{N} \{U_i + k_B T[x_{A,i} \ln x_{A,i} + (1 - x_{A,i}) \ln(1 - x_{A,i})]\} \tag{2.1}$$

where $x_{A,i}$ is the concentration of component A of the alloy in the ith layer parallel to the surface and U_i is approximated by the electronic contribution

$$U_i = \int_{-\infty}^{E_F} \mathrm{d}E\, E\rho_i(E; \{x_{A,j}\}, \{\alpha_j\}). \tag{2.2}$$

In equation (2.2), ρ_i is the average density of states for an atom in the ith layer. The density ρ_i of states depends on the concentration $x_{A,i}$ in the ith layer ($j = i$) and on the concentrations in all the other layers ($j \neq i$). In addition, ρ_i can depend on the potentials α_j which are different for the various layers. The potentials α_j are introduced to secure the neutrality of each crystal layer against the effect of the surface and/or a change in the concentrations of the components of the alloy in the ith crystal layer in relation to the bulk composition.

Equation (2.1) can be supplemented with a phonon term [21]. The calculation of the phonon term requires, however, the introduction of additional adjustable parameters [21] and it will be neglected in the present calculations.

When the free energy has been calculated, the equilibrium concentrations $x_{A,i}$ in the layers affected by the presence of the surface can be obtained from the condition [18]

$$(\partial F/\partial x_{A,i})_{x_{A,j\neq i}=\text{constant}} = (\partial F/\partial x_{A,m})_{x_{A,j\neq m}=\text{constant}} \tag{2.3}$$

where the derivative with respect to $x_{A,i}$ is taken for fixed concentrations $x_{A,j}$ of all other layers and m denotes a layer in the bulk.

2.1. *Calculation of the electronic contribution U_i*

In order to calculate the electronic contribution U_i to the free energy, the densities ρ_i of states for each crystal layer have to be found. We first consider the model based on additional assumptions that the density of states of d electrons can be described by the simple Hamiltonian in the tight-binding form and that the single hopping integral between lattice sites occupied by components A and B of the alloy fulfils the relation

$$t_{AA} = t_{AB} = t_{BB}. \tag{2.4}$$

The generalisation of the method for a more realistic Hamiltonian under the assumption that non-diagonal disorder can be neglected is straightforward and is discussed in § 4. The method can be also generalised for the case when $t_{AB}^2 = t_{AA}t_{BB}$ using the method described in [47, 48].

For a crystal with the surface described by the single-band Hamiltonian with diagonal disorder the CPA leads to the following set of coupled equations for the self-energy [49]:

$$x_{A,i}[\varepsilon_A - \Sigma_i(z)]/\{1 - [\varepsilon_A - \Sigma_i(z)]F_i(z)\} + x_{B,i}[\varepsilon_B - \Sigma_i(z)]/\{1 - [\varepsilon_B - \Sigma_i(z)]F_i(z)\} = 0 \tag{2.5}$$

where ε_A and ε_B are the atomic levels of components A and B, respectively, $x_{A,i}$ and $x_{B,i}$ are concentrations (atomic fractions) of the components A and B in the ith crystal layer parallel to the surface, $\Sigma_i(z)$ is the self-energy for the ith crystal layer and $F_i(z)$ is the matrix element of the Green function:

$$F_i(z) = \langle ni|\hat{R}(z)|ni\rangle \tag{2.6}$$

$$\hat{R}(z) = 1/[z - \hat{K}(z)] \tag{2.7}$$

$$\hat{K}(z) = \sum_{nj} \Sigma_j(z) c_{nj}^{+} c_{nj} + \hat{W} \tag{2.8}$$

$$\hat{W} = \sum_{nj} \alpha_j c_{nj}^{+} c_{nj} + t \sum_{nj\neq ml} c_{nj}^{+} c_{ml}. \tag{2.9}$$

In equations (2.6)–(2.9), $|ni\rangle$ denotes the Wannier state localised on a lattice site n belonging to the ith crystal layer, c_{ni}^{+} and c_{ni} are the creation and annihilation operators, respectively, for the Wannier state localised on the lattice site ni, and t is the hopping integral between nearest-neighbour lattice sites. The operator $\hat{W}$ also contains the additional potentials α_j assumed to be the same for both components A and B and introduced to ensure the neutrality of each crystal layer.

Equations (2.5) are coupled equations because $F_i(z)$ depends not only on Σ_i but also on the self-energies Σ_j for all other lattice layers. The number of equations depends on

how many crystal layers are assumed to be affected by the presence of the surface. The simplest decoupling scheme that can be introduced to solve the set of equations (2.5) consists of the assumption that

$$F_i(z) = F_i^0(z - \Sigma_i) \tag{2.10}$$

where

$$F_i^0(z) = \langle ni|(z - \hat{W})^{-1}|ni\rangle. \tag{2.11}$$

Equation (2.10) is exact for the bulk crystal and is equivalent for $\alpha_i = 0$ to the homogeneous decoupling approximation introduced in [49]. Moreover, the above relations are also exact if the Green function $F_i(z)$ is calculated with accuracy up to the second moment.

Equations (2.5)–(2.11) constitute the simplest calculation scheme of the electronic contribution to the free energy in the scope of CPA. However, it can easily be generalised if we realise that using equation (2.10) we can calculate the matrix element of the Green function for the Hamiltonian

$$\hat{K}_i^0 = \sum_{nj} \Sigma_i c_{nj}^+ c_{nj} + \hat{W} \tag{2.12}$$

instead of the Hamiltonian $\hat{K}$ given by equation (2.8). The difference between $\hat{K}$ and $\hat{K}_i^0$ which is given by

$$\hat{K}_i^1 = \sum_{j \neq i} (\Sigma_j - \Sigma_i) c_{nj}^+ c_{nj} \tag{2.13}$$

can be regarded as the perturbation and the Green function for the Hamiltonian $\hat{K}$ can be obtained with the aid of the perturbation theory. However, a more promising way for going beyond the homogeneous decoupling approximation seems to be the method based on the approximation corresponding to the rigid-band approximation for bulk crystals. If we assume that

$$\Sigma_j - \Sigma_i \simeq \varepsilon_j - \varepsilon_i \tag{2.14}$$

for $j \neq i$, the Hamiltonian $\hat{K}_i^1$ can be included in the operator $\hat{W}$ and the Green functions F_i^0 and F_i can be obtained with the aid of an iterative procedure.

Since the matrix elements $F_i^0(z)$ are related to the local densities $\rho_i(E)$ of states for the ith layer by the standard formula

$$F_i^0(z) = \int_{-\infty}^{+\infty} \mathrm{d}E\,(z - E)^{-1} \rho_i(E) \tag{2.15}$$

the calculation scheme based on equations (2.5)–(2.11) requires knowledge of ρ_i for the bulk crystal and all crystal layers affected by the presence of the surface. The density of states for the bulk crystal can be assumed to be either the realistic density of states for the alloy constituent or any model density of states approximating the density of states of alloy constituent. A very convenient way to construct the density of states for the crystal layers affected by the presence of the surface and/or the potential α_i is the

modified moments method [50, 51]. The density $\rho_i(E; \alpha_i)$ of states can thus be calculated at various levels of accuracy:

$$\rho_i(E; \alpha_i) = \omega(E) \sum_{n=0}^{N} \nu_n p_n(E) \tag{2.16}$$

where ν_n is the nth modified moment and p_n is the orthogonal polynomial defined by the weight function $\omega(E)$, and the Green function F_i can be easily calculated with the use of equation (2.15) for ρ_i given by equation (2.16).

Independently of the form of ρ_i used in the calculation the CPA equations lead to the Green functions for the ith layer of the alloy. The density $\rho_i(E; x_{A,i}, \alpha_i)$ of states for the ith layer of the alloy can then be calculated:

$$\rho_i(E; x_{A,i}, \alpha_i) = -\pi^{-1} \operatorname{Im}\{F_i^0[z - \Sigma_i(z)]\} \tag{2.17}$$

where $z = E + i\varepsilon$ and the limit $\varepsilon \to 0$ is taken.

The density of states for the ith layer depends on concentrations of alloy components and on the potential α_i for the ith layer. The potentials α_i are determined self-consistently from the Friedel-like local neutrality condition

$$\int_{-\infty}^{E_F} \mathrm{d}E\, \rho_i(E; x_{A,i}, \alpha_i) = x_{A,i} N_A + (1 - x_{A,i}) N_B. \tag{2.18}$$

It should be mentioned that the condition (2.18) is used both for the surface layer and for a layer in the bulk with the concentration $x_{A,i} \neq x_{A,b}$. The density $\rho_m(E; x_{A,m} + \Delta x, \alpha_m)$ of states where m denotes a layer in the bulk is needed in the calculation of $\partial U_b / \partial x_{A,m}$. The constraint (2.18) imposed in this way secures the neutrality of each crystal layer against the effect of the surface and/or a change in the concentrations of components of the alloy with respect to the bulk composition.

Equations (2.5)–(2.18) are generalised for the realistic density of states of the alloy in § 4. However, in order to show the effect of the local neutrality condition on the segregation and the general features of the segregation curves which can be obtained from the model based on d-band contributions, we start the calculations assuming a simple model density of states for the bulk crystal and the surface layer.

3. Model calculations

We start the calculation of the surface segregation assuming the simple model density of states for the ith crystal layer in the form

$$\rho_i(E; \alpha_i) = (b_i/2\pi)(1 - E^2)^{1/2}[(\tfrac{1}{4} - b_i)E^2 - (\tfrac{1}{2} - b_i)\alpha_i E^2 + b_i^2 + (\alpha_i/2)^2]^{-1} \tag{3.1}$$

where

$$b_i = \mu_{2i} - \alpha_i^2. \tag{3.2}$$

μ_{2i} is the second moment of the density of states for the ith crystal layer and the energy scale was assumed so that the band width is equal to 2. The model density of states is accurate up to the second moment and was previously used in the calculation of the surface relaxation [52]. If the accuracy is limited to the second moment, the only layer affected by the presence of the low-index surface plane (except for (110) plane for the FCC lattice and the (111) plane for the BCC lattice) is the surface layer.

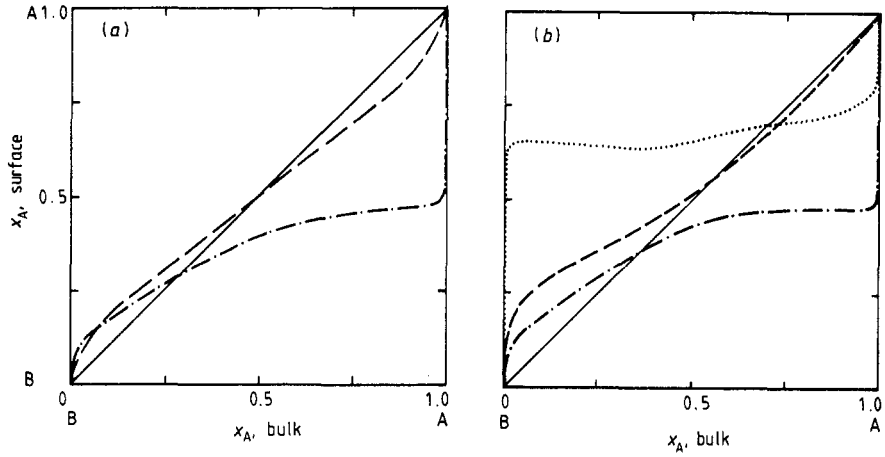

Figure 1. (*a*) Surface segregation at the (001) surface plane of a FCC alloy at 300 K where the d-band filling for both of the alloy components is equal to 5 and $\delta = -0.25$ (in units of half-band width; the band width is assumed in all present calculations to be equal to 4 eV): ———, results for potentials $\alpha_j = 0$; — · —, results for potential α_i calculated from the neutrality condition (2.18). (*b*) The same as (*a*) but for $N_A = 6$, $N_B = 5$ and $\delta = -0.40$: · · · ·, results obtained with the neutrality condition used in [23].

CPA equations for the bulk crystal and for the surface layer together with the local neutrality constraint form the set of equations which fully determines the density of states for the ith layer of the alloy and the d-band contribution U_i to the free energy of the system. The derivative $\partial U_i/\partial x_{A,i}$ can be calculated partly analytically for the simple model considered in this section.

The density ρ_i of states fulfils symmetry relations [32] with respect to the concentrations of alloy components. They lead to particularly simple symmetry properties of the derivative of the free energy in the case when both components have a half-filled d band ($N_A = N_B = 5$):

$$(\partial F/\partial x_{A,i})|_{x_{A,i}=c} + (\partial F/\partial x_{A,i})|_{x_{A,i}=1-c} = (\partial/\partial c)\,\mu_1^{(i)}(c) \tag{3.3}$$

where

$$\mu_1^{(i)}(c) = \varepsilon_A c + \varepsilon_B(1-c) + \alpha_i. \tag{3.4}$$

If $\alpha_i = 0$ for all crystal layers, equation (3.3) leads to the segregation curve which has a crossover for $x_{A,b} = 0.5$ and the upper part of the curve (for $x_{A,b} > 0.5$) can be obtained from its lower part by two succeeding mirror reflections with respect to the straight lines: $x_{A,i} = x_{A,b}$ and $x_{A,i} = 1 - x_{A,b}$.

The calculation scheme based on the density of states in the form (3.1) was first applied to the hypothetical alloy for which both components have a half-filled d band ($N_A = N_B = 5$). The alloy is assumed to form the crystal of the FCC symmetry with the (001) surface plane. This assumption determines the number of dangling bonds for an atom at the surface to be one third of the number of nearest neighbours. The surface plane is the only plane affected by the presence of the surface in the approximation considered. The calculations were performed for $\delta = \varepsilon_A - \varepsilon_B = -0.25$. The results are shown in figure 1(*a*). The broken curve represents the segregation curve for the case for

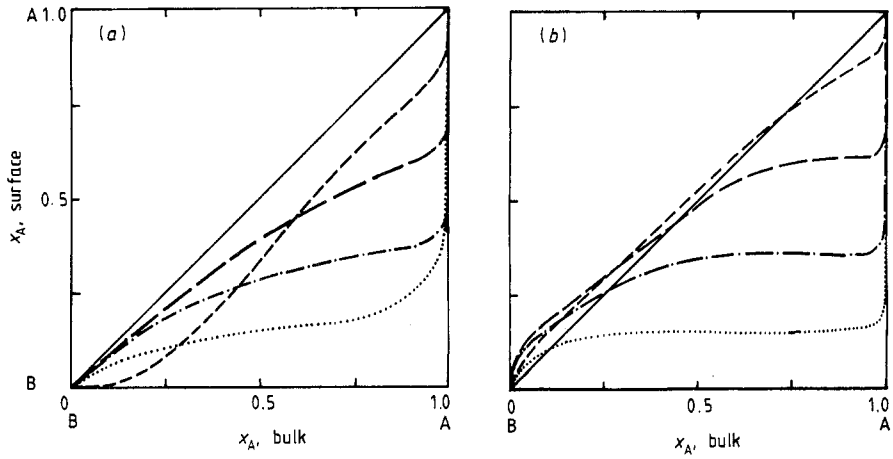

Figure 2. (*a*) Surface segregation at the (001) surface plane of a FCC alloy at 600 K for $\delta = -0.25$ and $N_A = N_B + 1$: ———, $N_B = 8$; ———, $N_B = 6$; — · —, $N_B = 4$; · · · ·, $N_B = 2$. (*b*) The same as (*a*) but for $\delta = -0.40$.

which the constraint (2.18) is not imposed, the potentials α_j are put equal to zero, and the surface and/or concentration changes disturb the neutrality of the crystal layer. The segregation curve in this case shows the symmetry properties discussed above. If the neutrality condition (2.18) is imposed, the segregation curve loses its simple symmetry properties and takes on the shape of the chain curve shown in figure 1(*a*). Comparison of these two curves in the figure shows that the neutrality constraint ignored in [18, 21] has considerable effect and should not be neglected in the calculation of the electronic contribution to the free energy. A similar comparison is presented in figure 1(*b*) for $N_A = 6$ and $N_B = 5$. The third curve in the figure (the dotted curve) is obtained when the neutrality constraint is imposed in the manner suggested in [20, 23] (the neutrality condition imposed in this way does not give any effect for $N_A = N_B$). Figure 1(*b*) shows that the way in which the neutrality constraint is imposed is also important. The sensitivity of the segregation on the neutrality condition also explains the discrepancy between results reported in [23, 28] obtained from the same model but with different neutrality constraints.

The model considered contains three parameters: the d-band fillings N_A and N_B of alloy components and the d-level splitting δ. It can be expected that the model in which hopping integrals have the same value independently of which atoms occupy neighbouring lattice sites will work better for metals for which the d-band fillings are close to each other. The d-level splitting $\delta = \varepsilon_A - \varepsilon_B$ for metals belonging to the same transition-metal series can be expected to be negative for $N_A > N_B$ [53]. Figures 2 and 3 illustrate the effect of band filling and d-level splitting on the segregation for $N_A = N_B + 1$ and $\delta < 0$. The figures show that both types of curve which cross and do not cross the no-segregation straight line can be obtained for different values of d-level splitting. The crossover occurs for smaller values of δ (for greater absolute values) and shifts towards a larger bulk concentration of component A when N_A increases. Figure 4 shows the effect of the different surfaces on the segregation. As could be expected, the segregation increases when the number of dangling bonds increases and the segregation

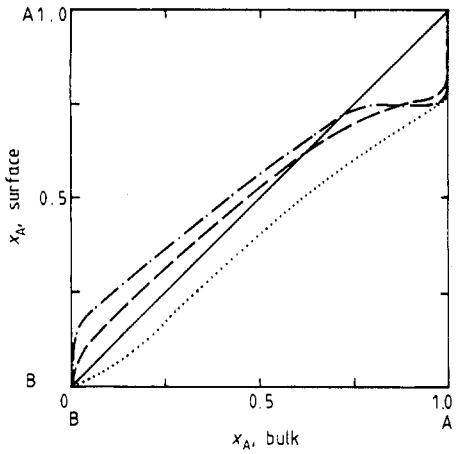

Figure 3. Surface segregation at the (001) surface plane of a FCC alloy at 600 K for $N_A = 8$ and $N_B = 7$: · · · ·, $\delta = -0.25$; — — —, $\delta = -0.40$; — · —, $\delta = -0.60$.

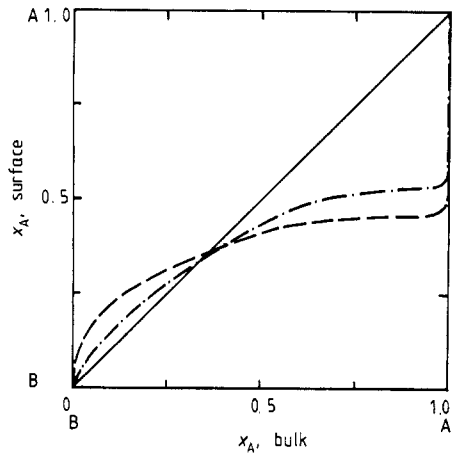

Figure 4. Surface segregation of a BCC alloy (eight nearest neighbours) at 600 K for $\delta = -0.25$ and $N_A = N_B + 1 = 6$: — — —, (001) or (111) surface plane (four dangling bonds); — · —, (110) surface plane (two dangling bonds).

is significantly changed for the (001) surface plane of the BCC lattice (four dangling bonds) in comparison with the (110) surface plane (two dangling bonds).

The effect of temperature is not very large. The calculations performed for the (001) surface plane of the BCC lattice, $\delta = -0.25$, $N_A = N_B + 1 = 6$ and $T = 700$ K give surface compositions which differ by less than 0.3% from those obtained for $T = 600$ K. This could be partly connected with the fact that in the present model the temperature enters only through the entropy term and all other effects which can be caused by a temperature change are neglected.

The description of a real system is not the aim of the calculation presented in this section. However, it can be expected that the model based on the simple density of states will work for d-band fillings close to one half. Both the model density of states and the realistic densities of states assume relatively large values in the vicinity of the Fermi levels for such cases and this leads to similar behaviours in the process of the calculation of the surface potentials. Also alloys composed of metals lying in the middle of the first transition-metal series tend to crystallise in a BCC lattice [54] and the d-band density of states for the BCC lattice in the nearest-neighbour approximation is symmetrical with respect to $E = 0$ in a similar way to the model density of states. For these reasons, experimental data for Cr–Fe and Co–Fe were chosen for comparison with results obtained for the model density of states. Figures 5 and 6 show the comparisons for Cr–Fe and Co–Fe alloys, respectively, for values of δ adjusted to obtain the best fits to the experimental data [55]. The sign of δ is in agreement with δ estimated from the work functions for Cr, Fe and Co [53]. The adjustment of δ allowed us to obtain a qualitative fit to experimental data; however, it should be mentioned that the increase in δ to 0.20 in the case of the Cr–Fe alloys and the decrease in δ to -0.25 in the case of the Co–Fe alloys leads to the crossover for large bulk concentrations of Cr in the case of Cr–Fe alloys and for large bulk concentrations of Fe in the case of Co–Fe alloys. It should also be mentioned that the model density of states can be expected to work better for middle

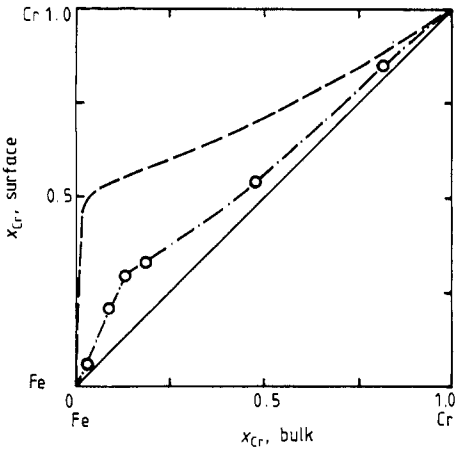

Figure 5. Surface segregation for Cr–Fe alloys at 650 K: ———, present model for $\delta = \varepsilon_{Cr} - \varepsilon_{Fe} = 0.18$, and $N_{Cr} = 5$ and $N_{Fe} = 6.4$ is assumed in agreement with [56]; — · —, experimental data taken from [55]. The other available experimental results [57–59] agree qualitatively with the data presented in the figure.

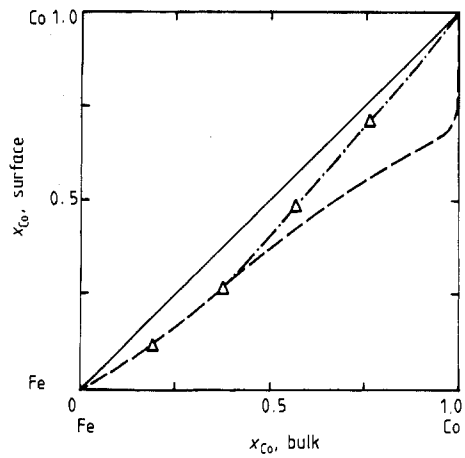

Figure 6. Surface segregation for Co–Fe alloys at 650 K: ———, present model for $\delta = \varepsilon_{Co} - \varepsilon_{Fe} = -0.22$, $N_{Co} = 7.9$ and $N_{Fe} = 6.4$; — · —, experimental data [55] (the data reported in [60] and [61] are in qualitative agreement with those shown in the figure).

alloy compositions. The process of alloying leads to a smooth density of states in this region of concentrations and all details of the densities of states of alloy components may be less important.

The method described in § 2 makes it possible to use more realistic densities of states for alloy components. This possibility is particularly important for the calculation of the segregation in alloys with a nearly filled d band. We take advantage of this possibility in the following section.

4. Calculations for Cu–Ni alloys

Now, we assume that the electronic structure of the alloy is described by a more realistic Hamiltonian of the form

$$\hat{H} = \hat{D} + \hat{W} \tag{4.1}$$

where

$$\hat{D} = \sum_{\mu,in} \varepsilon_{\mu,in} c^{+}_{\mu,in} c_{\mu,in} \tag{4.2}$$

is diagonal and configurationally dependent and

$$\hat{W} = \sum_{\substack{in \neq jm \\ \mu,\nu}} t_{\mu,in;\nu,jm} c^{+}_{\mu,in} c_{\nu,jm} + \sum_{\mu,in} \alpha^{+}_{i} c^{+}_{\mu,in} c_{\mu,in} \tag{4.3}$$

is the configurationally independent part of the Hamiltonian. In equations (4.2) and (4.3), $c^{+}_{\mu,in}$ and $c_{\mu,in}$ are the creation and annihilation operators, respectively, for the

Wannier state of μ symmetry ($\mu = 1, 2$ or 3 correspond to d orbitals of t_{2g} symmetry and $\mu = 4$ or 5 correspond to d orbitals of e_g symmetry). In a similar way to in [62], the hopping integrals $t_{\mu,in,\nu jm}$ between orbitals μ and ν localised on sites n and m in crystal layers i and j are assumed to be independent of which atoms occupy the sites in and jm. $\varepsilon_{\mu,in}$ is equal to the atomic level ε_A if the site in is occupied by atom A and is equal to ε_B otherwise (it is assumed that ε_A and ε_B have the same values for orbitals of e_g and t_{2g} symmetry). The Hamiltonian (4.1) differs from that used in [62] by the presence of diagonal potentials α_i introduced in a similar way to previously to secure the neutrality of each crystal layer against the effect of the surface and/or a change in the concentrations of components of the alloy in the ith crystal layer in relation to the bulk composition.

For the Hamiltonian (4.1) the CPA leads to a similar set of coupled equations to those considered in § 2. The only difference is that the set of equations is now doubled; we obtain separate equations for two symmetry components Σ_i^λ ($\lambda \equiv e_g$ or t_{2g}) of the self-energy for the ith crystal layer:

$$x_{A,i}[\varepsilon_A - \Sigma_i^\lambda(z)]/\{1 - [\varepsilon_A - \Sigma_i^\lambda(z)]F_i^\lambda(z)\} + x_{B,i}[\varepsilon_B - \Sigma_i^\lambda(z)]/\{1 - [\varepsilon_B - \Sigma_i^\lambda(z)]F_i^\lambda(z)\} = 0 \tag{4.4}$$

where F_i^λ is the λ-symmetry component of the diagonal matrix element of the Green function

$$F_i^\lambda(z) = \langle ni|\hat{P}_\lambda \hat{R}(z)|ni\rangle \tag{4.5}$$

$\hat{P}_\lambda$ is the projection operator selecting the subspace of states having λ symmetry and $\hat{R}$ is the Green function corresponding to the effective Hamiltonian

$$\hat{K}(z) = \sum_{\lambda,ni} \Sigma_i^\lambda(z) c_{\lambda,ni}^+ c_{\lambda,ni} + \hat{W}. \tag{4.6}$$

The set of equations (4.4) is the generalisation of CPA equations derived in [62] for the case when crystal layers can differ because of the presence of the surface and reduces to the equations used in [62] for the bulk crystal and α_i equal to zero.

Equations (4.4) are coupled with respect to t_{2g} and e_g symmetry components of the self-energy as well as to the layer indices. In order to solve the complicated set of CPA equations the following simplifying approximation is introduced. We assume that F_i^λ can be calculated from the formula

$$F_i^\lambda(z) = F_{A,i}^\lambda\{z - [\Sigma_i^\lambda(z) - \varepsilon_A]\} \tag{4.7}$$

where A is the major component of the alloy and $F_{i,A}$ is the Green function matrix element for component A and ith crystal layer. The approximation (4.7) incorporates both the homogeneous decoupling approximation and the t_{2g}–e_g decoupling approximation. The latter is justified by the relatively small mixing of t_{2g} and e_g states in pure Ni and Cu crystals and was successfully used in [63] to obtain the Cu–Ni alloy density of states for a wide range of alloy compositions. We also assume that the presence of the surface affects only one crystal layer, i.e. the surface plane, and that the concentrations of alloy components can differ from their bulk values only in the surface plane.

The Green function matrix element $F_{A,i}^\lambda(z)$ occurring on the right-hand side of equation (4.7) can be calculated from the standard formula

$$F_{A,i}^\lambda(z) = \frac{1}{n_\lambda}\int_{-\infty}^{+\infty} \frac{\rho_{A,i}^\lambda(E;\alpha_i)}{z - E}\,dE \tag{4.8}$$

where $\rho_{A,i}^\lambda$ is the λ-symmetry component of the density of states for a pure A (major)

component of the alloy, i denotes either the bulk or the surface layer, n_λ is the number of states of λ symmetry ($n_{t_{2g}} = 3, n_{e_g} = 2$) and the density of states depends on the potential α_i.

In order to start the calculation by the CPA method, we need densities $\rho^\lambda_{A,i}$ of states for the bulk layer with $\alpha_i = 0$ and $\alpha_i \neq 0$ (required for the calculation of the derivative $\partial U_b/\partial x_{A,i}$) and for the surface layer, $\rho^\lambda_{A,b}(E; 0)$ were obtained using the hopping integrals for the d band given in [64] for both Cu and Ni. The method used to obtain two symmetry components of the density of states was the method suggested in [65] adapted for the FCC lattice (see Appendix). Then, in a similar way to in [62], the components of the density of states were approximated by the straight-line segments (using 100 segments for the whole band). In this way, $F^\lambda_{A,b}$ for each segment is obtained in the analytical form [66]. The densities of states both for the surface layer and for the layer with $\alpha_i \neq 0$ were obtained by the modified moments method (equation (2.16)). The bulk density $\rho^\lambda_b(E; 0)$ of states for $\alpha = 0$ was used as the weight function in equation (2.16) for both $\rho^\lambda_s(E; \alpha_s)$ and $\rho^\lambda_b(E; \alpha_b)$. N in equation (2.16) was taken to be equal to 2. The expansion of the density of states in terms of orthogonal polynomials is certainly too short to reproduce all details of the surface density of states. However, since the density of states for the bulk is assumed to be the weight function, the first few terms of the expansion should correctly describe the effect of the surface on averages calculated over the density of states. It should be mentioned that the integration (4.8) can be analytically performed for each segment also in the case of modified densities of states and that the homogeneous decoupling approximation becomes exact in the case of the expansion (2.16) truncated at $N = 2$. The modified moments method can lead to a small unphysical negative value of the density of states for certain small regions of the energy. In such a case the density of states was taken to be equal to zero for such energy values and the whole density of states was renormalised.

As in the case of the model calculation the potentials α_i were determined self-consistently from a Friedel-like local neutrality condition.

4.1. Results and discussion

Figure 7 shows the surface composition as a function of the bulk composition for $T =$ 600 K and the (001) surface plane. The results have been obtained for $\delta = -0.40$ measured in half-band widths. It corresponds to the value of -0.82 eV for the Ni-rich region of bulk concentrations and such a value has been previously used in the calculation of the alloy density of states [62]. Since the width of the Cu d band is less than that for Ni, the value of δ corresponds to -0.61 eV for the Cu-rich region of bulk concentrations. The values of δ are also in quite good agreement with the values which can be calculated from data reported in [53].

The calculations of the segregation are performed for the density of states of the major component of the alloy. The calculations of the surface segregation performed for the nickel density of states for the whole region of bulk concentrations leave the segregation curve qualitatively unchanged and the maximum difference between the values of the surface composition obtained for density of states of the major and minor components of the alloy is less than 0.03 atomic fraction. Thus the use of the density of states of a major component of the alloy does not lead to a qualitative change in the character of the segregation curve.

Figure 7 also shows the dependence of the segregation on the Ni d-band filling. As can be seen, the dependence on d-band filling is relatively weak for the value of δ used

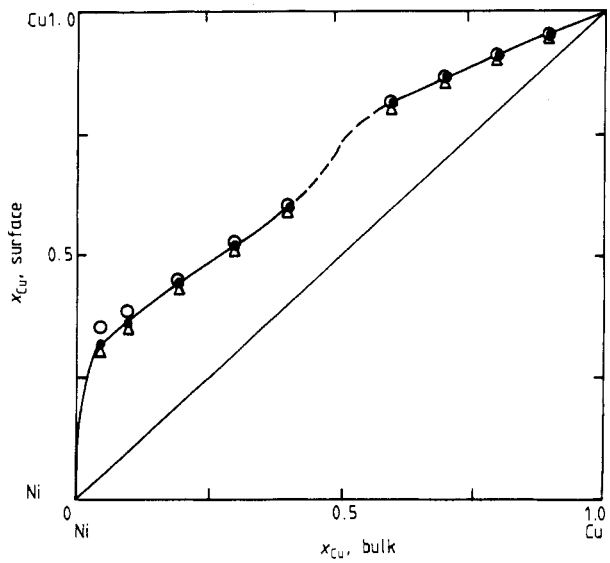

Figure 7. Surface segregation of Cu–Ni alloys at the (001) surface plane at 600 K for $\delta = -0.40$ (measured in half-band widths) and $N_{Cu} = 10$: ●, $N_{Ni} = 9.45$; △, $N_{Ni} = 9.55$; ○, $N_{Ni} = 9.35$.

in obtaining the results shown in figure 7 (as could be expected, the sensitivity of the surface composition on N_{Ni} decreases when x_{Cu} increases).

The comparison between the segregation calculated by the present method for $T = 850$ K and the experimental results is shown in figure 8 (most experimental results are obtained for a temperature range close to 850 K). As can be seen, the theoretical curve is in qualitative agreement with all experimental data except for those [44] which predict the crossover phenomenon for large bulk concentrations of copper. The segregation curve at present obtained also remains in qualitative agreement with the results of [23] and disagrees with the results of [28]. This point requires a short discussion. The methods used both in [28] and in the present paper include the neutrality constraint. The neutrality constraint is imposed in different ways. In [28] the band centres of alloy components are shifted to ensure neutrality and the condition that the constituent atoms of the alloy at the surface are electrically polarised in the same way as the bulk is imposed. On the other hand in the present paper the same surface potential is assumed for both alloy constituents. These ways of imposing the neutrality conditions are based on opposite approximations. The approximation used in the present calculation leaves the positions of d bands of alloy constituents unchanged as in the case of exact calculations for a crystal with a surface [67]. However, the different ways of imposing a neutrality condition do not seem to be the main reason for the discrepancy between our results and those of [28]. The derivative of the free energy with respect to the concentration in a layer in the bulk is calculated in [28] without a neutrality constraint (in our case the potential α was also used to ensure neutrality of a layer in the bulk in the calculation of the derivative). The manner of the calculation of the derivative for a layer in the bulk is probably the main source of the discrepancy. On the other hand it would also explain the qualitative agreement between our results and the results of [23]. The neutrality condition in the latter paper is introduced in a questionable way [68] but the calculations of derivatives

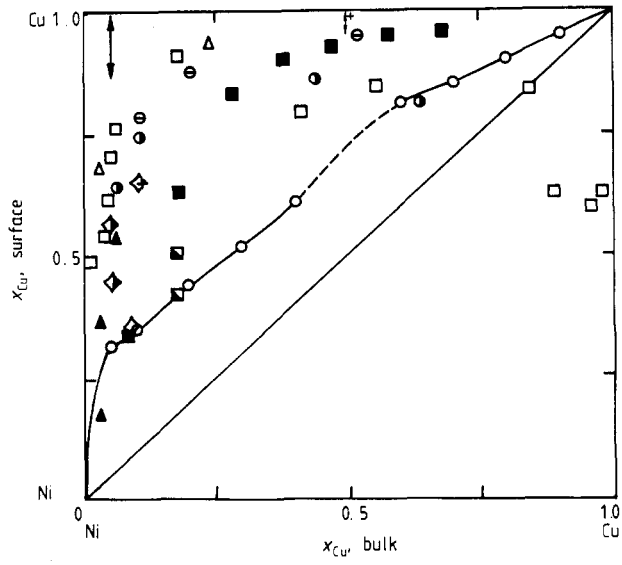

Figure 8. Comparison of calculated segregation curve (———) with experimental data (○, [33]; +, [34]; ■, [35]; ◇, [37]; ⊖, [38]; ▲, [39, 40]; ◙, [41]; ↕, [42]; ◆, [43]; □, [44]; △, [46]) for $\delta = -0.40$, the (001) surface plane and $T = 850$ *K*.

for a surface layer and a layer in the bulk are performed in a more consistent way (in both cases the neutrality condition is not imposed). Thus our results obtained for a realistic density of states seem also to confirm the conclusion derived in [30] for a very simple density of states that the neutrality condition does not lead to the crossover of the segregation curve for Cu–Ni alloys.

The question arises to what extent the results for Cu–Ni alloys are sensitive to the parameters of the model, i.e. δ and d-band fillings of alloy constituents. The results obtained for a model density of states show that surface segregation is sensitive to these parameters. The value of δ is the small difference between two large quantities and as such is difficult to calculate accurately. We can treat δ as the parameter of the model not only because of difficulties in its calculation but primarily because the segregation is obtained as the result of a very complicated inter-play between the effect of the surface and the effect of alloying governed by the values of δ. Since the effect of the surface is taken into account approximately, the value of δ even when calculated accurately may not be the best value to describe a real crystal.

Figure 9 shows the surface segregation for the alloy containing 5 at.% Cu as a function of δ. At the same time the segregation for the alloy containing 90 at.% Cu was calculated. The segregation of copper in the Cu-rich alloy decreases when the absolute value of δ increases but the crossover phenomenon does not occur. The crossover phenomenon also does not appear when the d-band filling of Ni decreased to as low as 9 electrons/atom.

The interesting feature of the curve shown in figure 9 is the strong dependence of the surface segregation on δ at around -0.4 eV. Figure 10 shows the surface segregation curve obtained for $\delta = -0.15$ measured in half-band widths (this value of δ corresponds to -0.31 eV for the Ni-rich region of bulk concentrations) for the whole region of the bulk concentrations. For this value of δ the segregation shows a very strong dependence

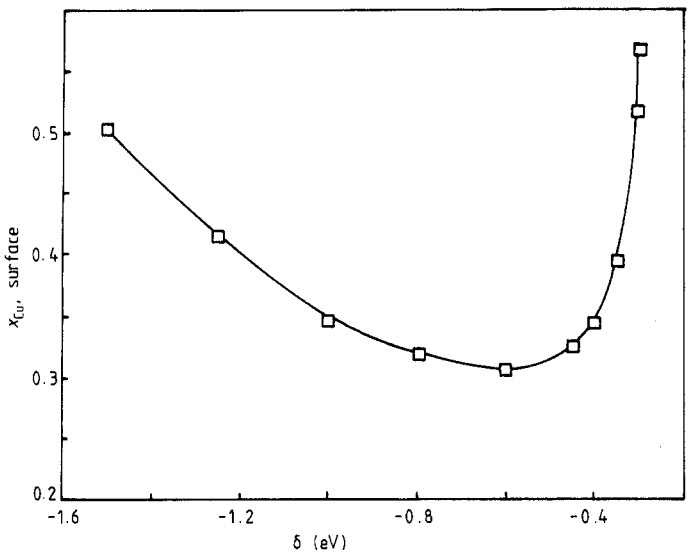

Figure 9. Surface segregation at 600 K as a function of parameter δ for $Cu_{0.05}Ni_{0.95}$ alloy.

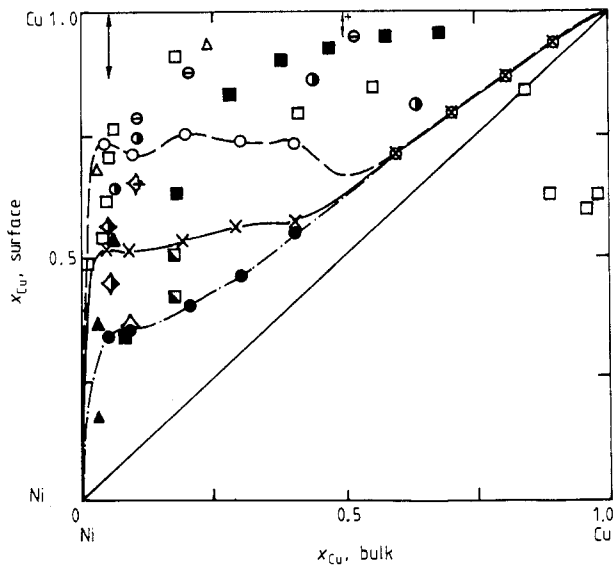

Figure 10. Surface segregation of Cu–Ni alloys at the (001) surface plane at 600 K for $\delta = -0.15$: ×, $N_{Ni} = 9.45$; ●, $N_{Ni} = 9.55$; ○, $N_{Ni} = 9.40$; the experimental data are denoted by the same symbols as in figure 8.

on the d-band filling in the Ni-rich region of bulk concentrations. The segregation curves have a very irregular shape in this region. This has a very simple explanation. The alloying process for a small value of δ leaves much of the band structure of alloy constituents unchanged, and the density of states at the Fermi level can change significantly with the change in d-band filling. The shape of the density of states in the

vicinity of the Fermi level probably plays an important role in the calculation of the surface segregation. If the model for a small value of δ describes the situation in the real crystal, this would explain the fact that experimental data are scattered for the Ni-rich region of bulk concentrations. The d-band filling can easily be changed by the presence of impurities and/or imperfections of the lattice in the alloy.

The calculated surface segregation particularly for $\delta = -0.40$ (figure 8) is much lower than experimentally observed. This discrepancy can stem from the approximation made in calculating the surface effect on the density of states, from neglecting other effects except for the d-band contribution and, in particular, from neglecting the Coulomb electron–electron interaction in calculating the electronic energy.

5. Summary and conclusions

We have performed calculations of the surface segregation by the CPA method both for a model density of states and for a realistic density of states of Cu–Ni alloys. The calculation of the effect of the surface required additional approximations, some of which can be removed (see discussion in § 2). The inclusion of other effects, such as surface relaxation, mismatch effects and lattice vibration would require introducing additional adjustable parameters.

The calculations performed for the model density of states have shown that the surface potential is very important in determining the surface segregation and that the model based on the d-band contribution to the segregation process predicts a qualitatively different behaviour of the surface segregation as a function of bulk composition depending on the d-band filling and on the d-level splitting of the alloy constituents. On the other hand the calculation performed for the realistic density of states of the Cu–Ni alloys predicts the segregation of copper for the whole region of bulk compositions and for all reasonable values of parameters and it does not seem very probable that a refinement of the model can lead to the crossover phenomenon. In the calculation of the alloy density of states for the bulk Cu–Ni crystal no other approximations have been introduced except for those used before in similar calculations [62]. The Hubbard term neglected in the present calculation shifts the crossover to a large value of Cu concentration [28] and the calculation [29] performed with the energy term suggested in [69] does not also predict the segregation of nickel. However, it should be mentioned that the present calculations are confined to d-band effects; the d band certainly plays a decreasing role in determining the surface segregation when the d-band filling increases. Therefore, for Cu-rich alloys, other effects such as the effects of the s band and the lattice vibrations can play a relatively more important role.

The calculation performed for the small absolute value of the d-band splitting shows a strong dependence of the segregation on the d-band filling for Ni-rich alloys. This could partly explain the disagreement with the experimental data for this region of alloy compositions.

Acknowledgment

One of us (PM) would like to thank the research project CPBP 01.08 for financial support.

Appendix

The evaluation of the energy surface integrals by the method in [65] requires the partition of the Brillouin zone (or its irreducible part) into small tetrahedra. The irreducible Brillouin zone (IBZ) for the SC lattice has the form of a simple tetrahedron and it can easily be divided into n^3 ($n = 2, 3, \ldots$) congruent tetrahedra. (Moreover, six such tetrahedra form a cube; so the IBZ can be first filled up as much as possible with cubes and then supplemented with tetrahedra located along edges or at the corners of the IBZ.)

The IBZ for a FCC lattice is a rather irregular polyhedron and it cannot be directly divided into congruent (or equivolume) tetrahedra. However, it can be decomposed into three tetrahedra [70], which can be obtained from IBZ for the SC lattice by suitably chosen linear transformations. The following transformations can be used:

$$\hat{\mathbf{T}}_1 = \begin{pmatrix} 2 & 0 & 0 \\ 0 & -\frac{1}{2} & -\frac{1}{2} \\ 0 & \frac{1}{2} & -\frac{1}{2} \end{pmatrix} \qquad \hat{\mathbf{T}}_2 = \begin{pmatrix} 2 & -\frac{1}{2} & -\frac{1}{2} \\ 1 & \frac{1}{2} & -\frac{1}{2} \\ 0 & 0 & 1 \end{pmatrix} \qquad \hat{\mathbf{T}}_3 = \begin{pmatrix} 2 & -1 & 1 \\ 1 & 0 & -\frac{1}{2} \\ 0 & 1 & -\frac{1}{2} \end{pmatrix}.$$

References

[1] Chelikovsky J R 1984 *Surf. Sci.* **139** L197
[2] Ossi P M 1988 *Surf. Sci.* **201** L519
[3] Kelley M J and Ponec V 1983 *Prog. Surf. Sci.* **11** 139
[4] Gijzeman O L J 1985 *Surf. Sci.* **150** 1
[5] Mezey L Z and Giber J 1985 *Surf. Sci.* **162** 514
[6] Williams F L and Nason D 1974 *Surf. Sci.* **45** 377
[7] Burton J J and Machlin E S 1976 *Phys. Rev. Lett.* **37** 1433
[8] Jabłoński A 1977 *Adv. Colloid Interface Sci.* **8** 213
[9] Donelly R G and King T S 1978 *Surf. Sci.* **74** 89
[10] Miedema A R 1978 *Z. Metallk.* **69** 455
[11] Crucq A, Degols L, Lienard G and Frennet A 1979 *Surf. Sci.* **80** 78
[12] Hamilton J C 1979 *Phys. Rev. Lett.* **42** 989
[13] Kumar V 1981 *Phys. Rev.* B **23** 3756
[14] Abraham F F and Brundle C R 1981 *J. Vac. Sci. Technol.* **18** 506
[15] Egelhoff W F Jr 1983 *Phys. Rev. Lett.* **50** 587
[16] King T S and Donelly R G 1984 *Surf. Sci.* **141** 417
[17] Foiles S M 1985 *Phys. Rev.* B **32** 7685
[18] Kerker G, Moran-Lopez J L and Bennemann K H 1977 *Phys. Rev.* B **15** 638
[19] Lambin Ph and Gaspard J P 1980 *J. Phys. F: Met. Phys.* **10** 2413
[20] Balseiro C A and Moran-Lopez J L 1980 *Phys. Rev.* B **27** 349
[21] Hoshino K 1981 *Proc. Phys. Soc. Japan* **50** 577
[22] Muscat J P 1982 *J. Phys. C: Solid State Phys.* **15** 867
[23] Mukherjee S, Moran-Lopez J L, Kumar V and Bennemann K H 1982 *Phys. Rev.* B **25** 730
[24] Riedinger R and Dreysse H 1983 *Phys. Rev.* B **27** 2073
[25] Masuda-Jindo K 1985 *Phys. Lett.* **107A** 185
[26] Yamauchi H 1985 *Phys. Rev.* B **31** 7688
[27] Foiles S M, Baskes M I and Daw M S 1986 *Phys. Rev.* B **33** 7983
[28] Lin H-F, Wang C L and Cheng Y-C 1986 *Solid State Commun.* **59** 253
[29] Desjonqueres M C and Spanjaard D 1987 *Phys. Rev.* B **35** 952
[30] Mukherjee S and Moran-Lopez J L 1987 *Surf. Sci.* **188** L742
[31] Soven P 1967 *Phys. Rev.* **156** 809
[32] Velický B, Kirkpatrick S and Ehrenreich H 1968 *Phys. Rev.* **175** 747
[33] Sinfelt J H, Carter J L and Yates D J C 1972 *J. Catal.* **24** 283

[34] Helms C R and Yu K Y 1975 *J. Vac. Sci. Technol.* **12** 276
[35] Watanabe K, Hoshiba M and Yamashina T 1976 *Surf. Sci.* **61** 483
[36] Kuijers F J and Ponec V 1977 *Surf. Sci.* **68** 294
[37] Ling D T, Miller J N, Lindau I, Spicer W E and Stephan P M 1978 *Surf. Sci.* **74** 612
[38] Brongersma H H, Sparnaay M J and Buck T M 1978 *Surf. Sci.* **71** 657
[39] Ng Y S, Tsong T T and McLane S B 1979 *Surf. Sci.* **84** 31
[40] Ng Y S, McLane S B and Tsong T T 1980 *J. Vac. Sci. Technol.* **17** 154
[41] Wandelt K and Brundle C R 1981 *Phys. Rev. Lett.* **46** 1529
[42] Webber P R, Rojas C E, Dobson P J and Chadwick D 1981 *Surf. Sci.* **105** 20
[43] Webber P R, Morris M A and Zhang Z G 1986 *J. Phys. F: Met. Phys.* **16** 413
[44] Sakurai T, Hashizume T, Kobayashi A, Sakai A, Hyodo S, Kuk Y and Pickering H W 1986 *Phys. Rev.* B **34** 8379
[45] Rehn L E, Hoff H A and Lamm N Q 1986 *Phys. Rev. Lett.* **57** 780
[46] Berghaus Th, Lunau Ch, Neddermeyer H and Rogge V 1987 *Surf. Sci.* **182** 13
[47] Shiba H 1971 *Prog. Theor. Phys.* **46** 77
[48] Jacobs R L 1973 *J. Phys. F: Met. Phys.* **3** 933
[49] Berk N F 1975 *Surf. Sci.* **48** 289
[50] Modrak P, Bergesen B and Liu K L 1980 *Solid State Commun.* **36** 499
[51] Brejnak M and Modrak P 1987 *Acta Phys. Pol.* A **71** 619
[52] Masuda K 1982 *Phys. Rev.* B **26** 5968
[53] Nordlander P, Holloway S and Norskov J K 1985 *Surf. Sci.* **136** 59
[54] Hume-Rothery W 1966 *The Structures of Alloys of Iron* (Oxford: Pergamon)
[55] Asami K and Hashimoto K 1984 *Corros. Sci.* **24** 83
[56] Moruzzi V L, Janak J F and Williams A R 1978 *Calculated Electronic Properties of Metals* (Oxford: Pergamon)
[57] Leygraf C, Hultquist G, Ekelund S and Eriksson J C 1974 *Surf. Sci.* **46** 175
[58] Ng Y S, Tsong T T and McLane S B Jr 1979 *Surf. Sci.* **84** 31
[59] Dowben P A, Grunze M and Wright D 1983 *Surf. Sci.* **134** L524
[60] Allié G, Lauroz C and Villeman P 1981 *Surf. Sci.* **104** 583
[61] Herschitz R and Seidman D M 1985 *Acta Metall.* **33** 1547
[62] Kirkpatrick S, Velický B and Ehrenreich H 1970 *Phys. Rev.* B **1** 3250
[63] Stocks G M, Williams R W and Faulkner J S 1971 *Phys. Rev.* B **4** 4390
[64] Johnston N A, Sholl C A and Smith P V 1983 *J. Phys. F: Met. Phys.* **13** 945
[65] Lehmann G and Taut M 1972 *Phys. Status Solidi* b **54** 469
[66] Ehrenreich M and Schwartz L M 1976 *Solid State Phys.* **31** 149 (New York: Academic)
[67] Kalkstein D and Soven P 1971 *Surf. Sci.* **26** 85
[68] Cheng Y-C 1986 *Phys. Rev.* B **34** 7400
[69] Allan G 1970 *Ann. Phys., Paris* **5** 169
[70] Holas A 1977 *J. Comput. Phys.* **23** 150